Calibration activities of Microwave Diagnostic Instruments in LHD

Tokihiko. Tokuzawa[1,2,3] on behalf of

R. Yanai[1], D. Nishimura[1], Y. Nagayama[1], K. Tanaka[1,3], T. Kinoshita[3], and LHD experiment group

[1] National Institute for Fusion Science, [2] SOKENDAI, [3] Kyusyu University

Acknowledgments

This study was supported in part by the Japan Society for the Promotion of Science KAKENHI (grant nos. 19H01880, 21H04973, 23H01161, and 23K25858), by a budgetary Grant-in-Aid from the National Institute for Fusion Science LHD project under the auspices of the NIFS Collaboration Research Program, and by the Collaborative Research Programs of the Research Institute for Applied Mechanics, Kyushu University. Additional support was provided by Japan/U.S. Cooperation in Fusion Research and Development.

Contents

- ECE
  - Previous work
  - Recent work
- Millimeter-wave back-scattering
  - Elimination of back-ground noise
- Phase contrast imaging (Forward scattering)
  - Absolute density fluctuation estimation

Large Helical Device (LHD)

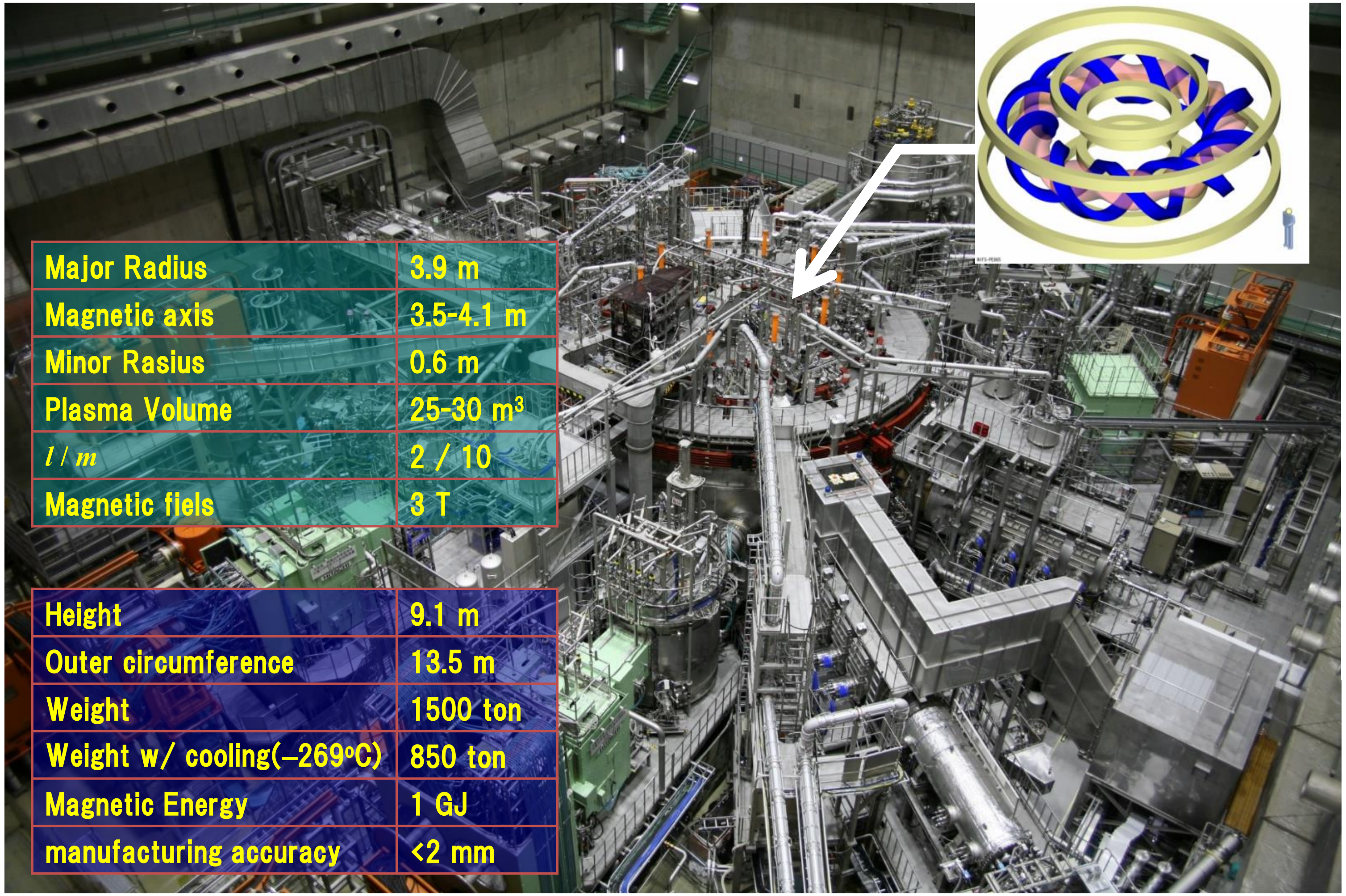

Major Radius	3.9 m
Magnetic axis	3.5-4.1 m
Minor Rasius	0.6 m
Plasma Volume	25-30 m^3
l / *m*	2 / 10
Magnetic fiels	3 T

Height	9.1 m
Outer circumference	13.5 m
Weight	1500 ton
Weight w/ cooling(–269°C)	850 ton
Magnetic Energy	1 GJ
manufacturing accuracy	<2 mm

Plasma parameters	Achievement
Ion temperature	120 million degrees (1.3×10^{19} /m^3)
Electron temperature	230 million degrees (0.2×10^{19} /m^3) 120 million degrees (1.6×10^{19} /m^3)
Electron density	1.2×10^{21} /m^3 (3 million degrees)
β value	5.1 % (0.425 T) 4.1 % (1.00 T)
Plasma duration	54 min. (0.5 MW) 48 min. (1.2 MW)

From 1998 to 2025, over 200,000 shots had been conducted for plasma science.

Magnetic field structure in LHD

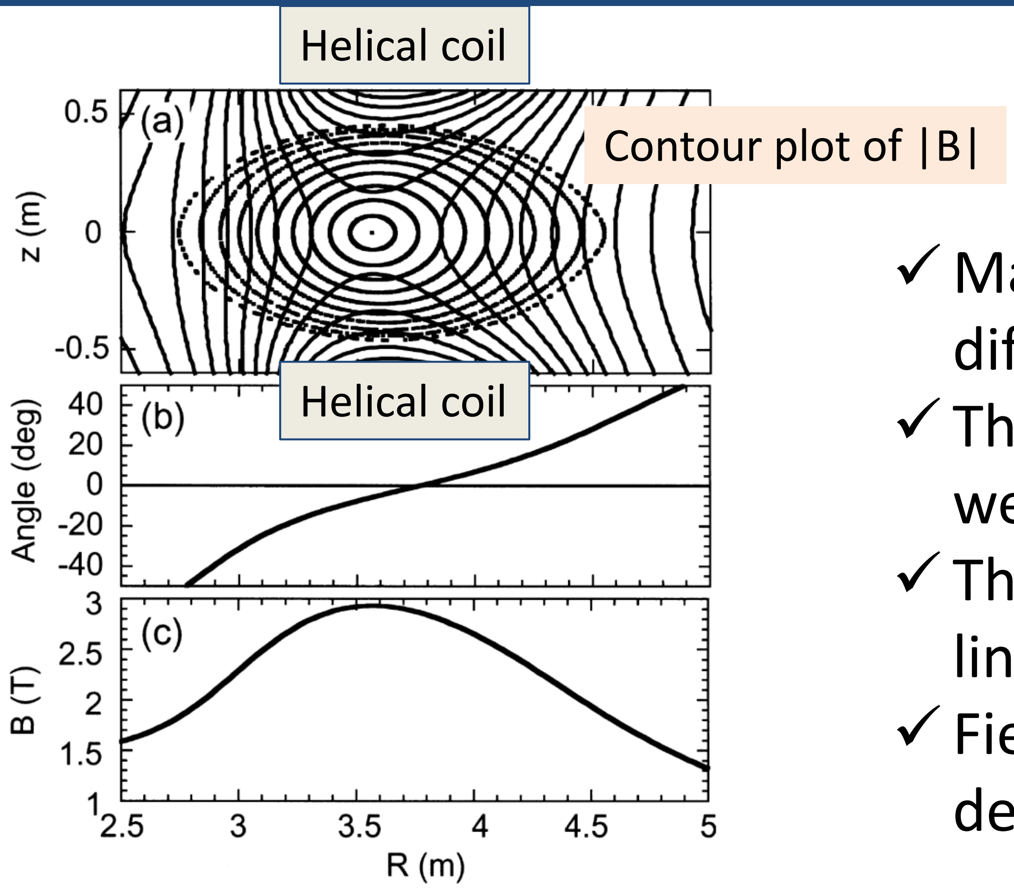

Fig. 1 (a) Contour plot of $|B|$ (solid contours) and flux surfaces (dotted contours) in the plasma cross-section. (b) Angle of the magnetic field. (c) Magnetic field on the viewing line of ECE diagnostics in the case of R_{ax} = 3.6 m and B_{ax} = 2.8 T in LHD.

- ✓ Magnetic field structure in LHD is different from tokamaks.
- ✓ The B is strongest at the coil and weakest at the port.
- ✓ The B profile is hill shaped in the view line of ECE antenna.
- ✓ Field angle changes from -40 to +40 degrees.

(previous) ECE systems in LHD

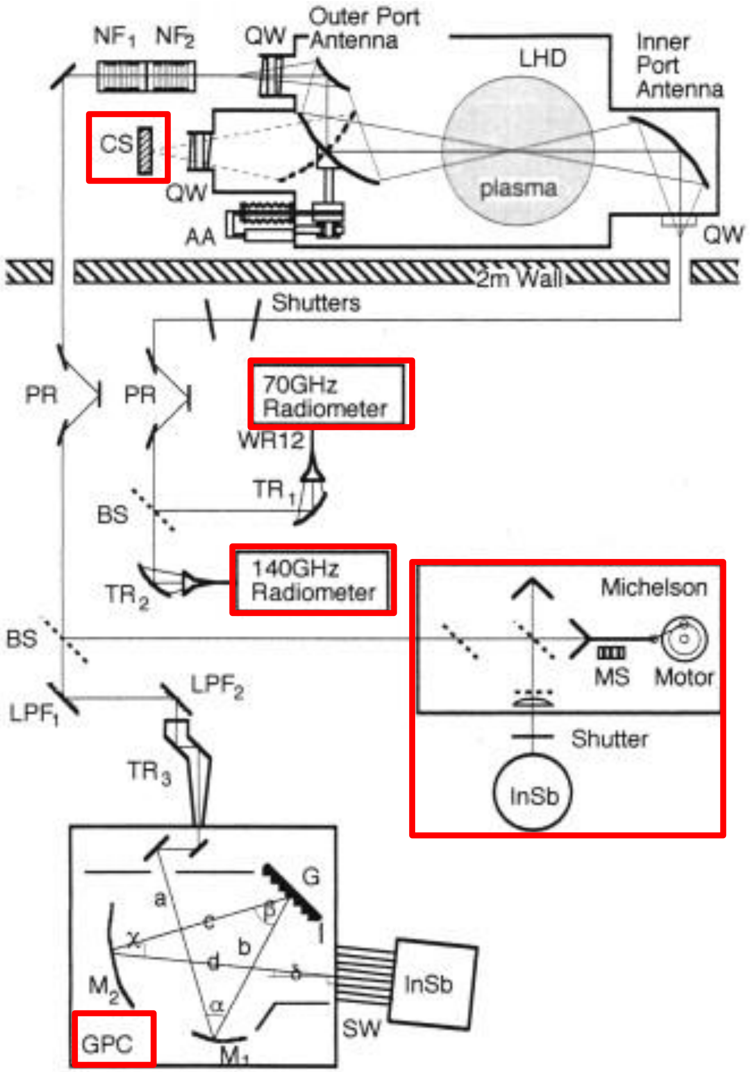

- ✓ ECE received by 2 antennas is transferred to the spectrum analyzers with the corrugated wave-guide system.
- ✓ **The Michelson system is absolutely calibrated**, and the radiometer and the GPC are cross-calibrated to the Michelson.

Fig. 3. Schematic diagram of the ECE diagnostic system in LHD. Each components are connected with 63.5 mm diameter corrugated waveguides. Symbols of components are as follows, QW, crystal quartz window; NF_1, 82.6 GHz Notch filter; NF_2, 84 GHz notch filter; AA, air actuator to rotate mirror; **CS, calibration radiation source**; PR, polarization rotator; BS, beam splitter; TR_1, transition from corrugated waveguide to WR12 rectangular waveguide; TR_2, transition from corrugated waveguide to WR8 rectangular waveguide; TR_3, transition from corrugated waveguide to WR8 rectangular waveguide; MS, Moire position sensor; LPF_1, 248 GHz low pass filter; LPF_2, 168 GHz low pass filter; G, grating; SW, short rectangular waveguide. Parameters of GPC are as follows, a=108.1 cm; b=87 cm; c=75 cm; d=70.5 cm; α=32°; β=34.5°; χ=38°; δ=9.9°.

Y. Nagayama+, Fusion Engineering and Design **53**, 201 (2001).

Previous calibration of ECE

ECE antenna

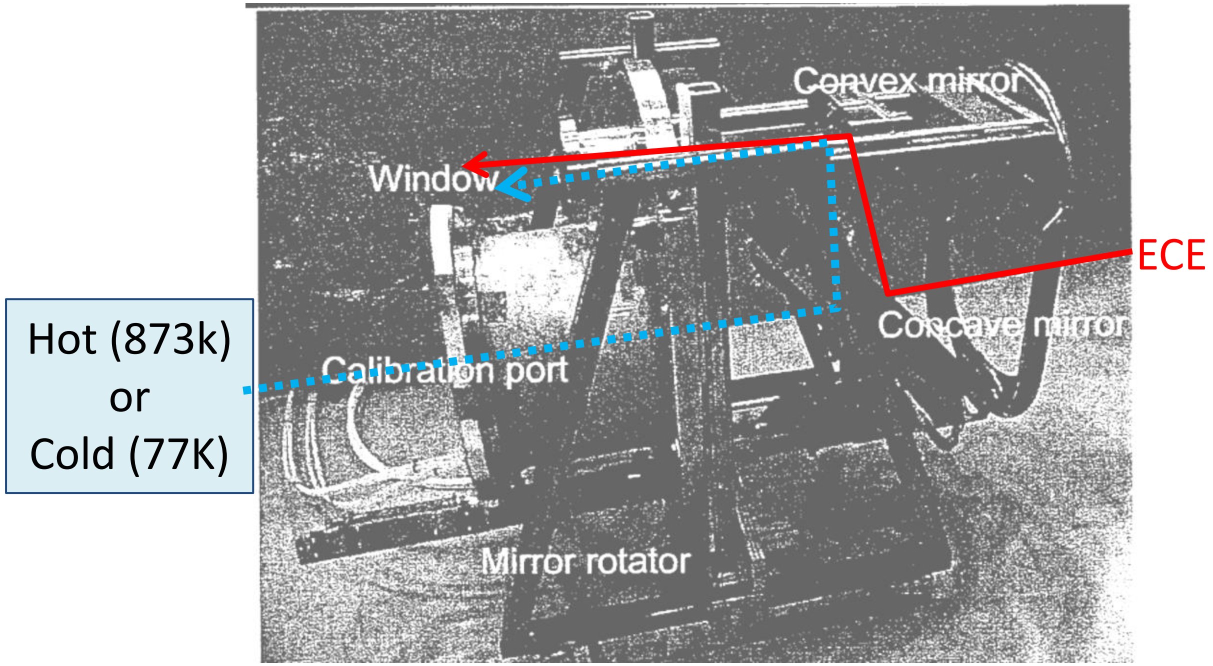

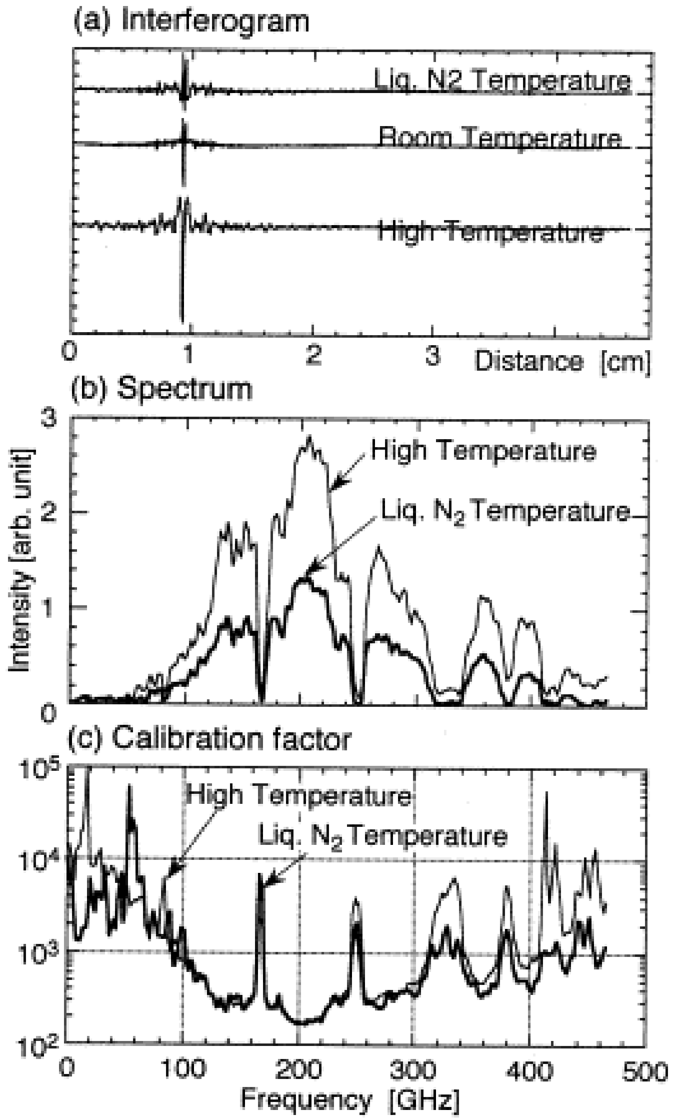

Fig. 11. (a) Interferograms of the microwave emission from the cold source cooled by the liquid nitrogen, then room temperature source and the hot source. (b) Spectra of the microwave emission from the cold source and the hot source. (c) CF obtained from the data of the cold source and the hot source.

Y. Nagayama+, Fusion Engineering and Design **53**, 201 (2001).

Comparison b/w ECE & TS

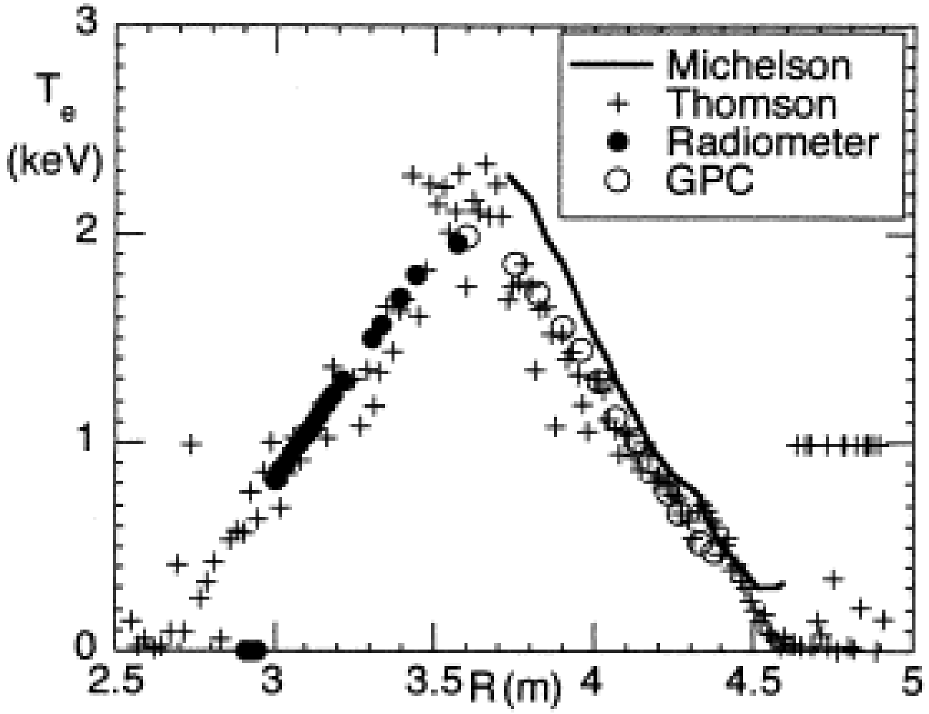

Fig. 12. Example of calibrated ECE spectrum obtained by the Michelson, the 70 GHz radiometer and the GPC. The electron temperature profile measured by the Thomson scattering is also shown.

Y. Nagayama+, Fusion Engineering and Design **53**, 201 (2001).

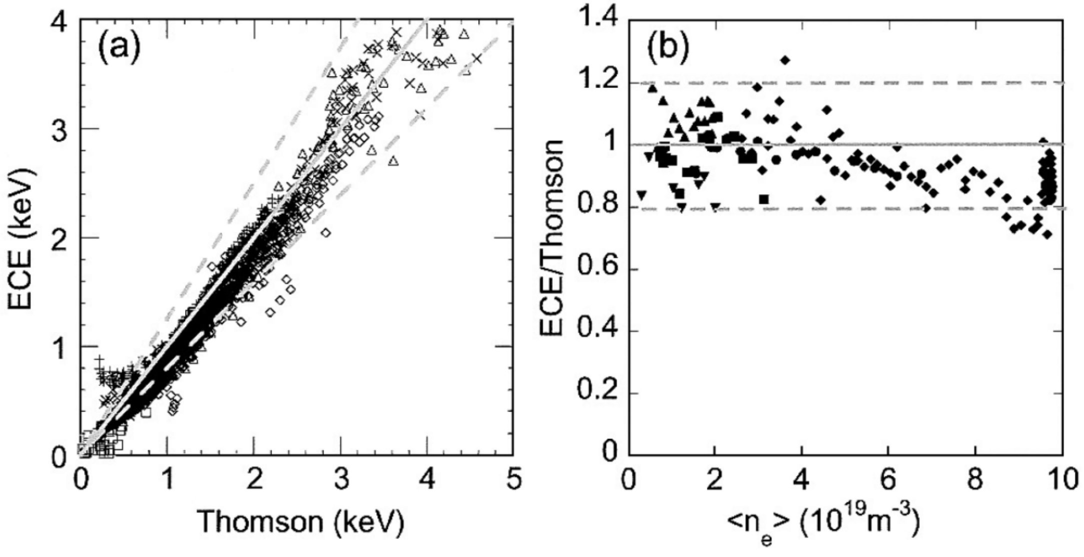

Fig. 8 (a) Comparison of the electron temperature measured with the Thomson scattering and the ECE diagnostics. (b) The ratio of the ECE and the Thomson scattering for the various lineaveraged electron densities. The gray line indicates $T_{ECE} = T_{Thomson}$. The broken lines indicate a discrepancy of ±20%.

Y. Nagayama+, J. Plasma Fusion Res. **79**, 6, 601 (2003).

Contents

- ECE
  - Previous work
  - Recent work
- Millimeter-wave back-scattering
  - Elimination of back-ground noise
- Phase contrast imaging (Forward scattering)
  - Absolute density fluctuation estimation

Recent ECE calibration

ECE port was MOVED

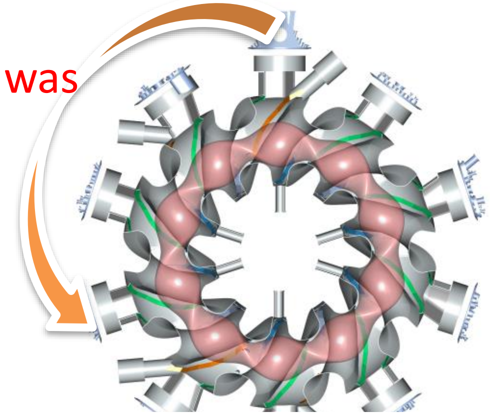

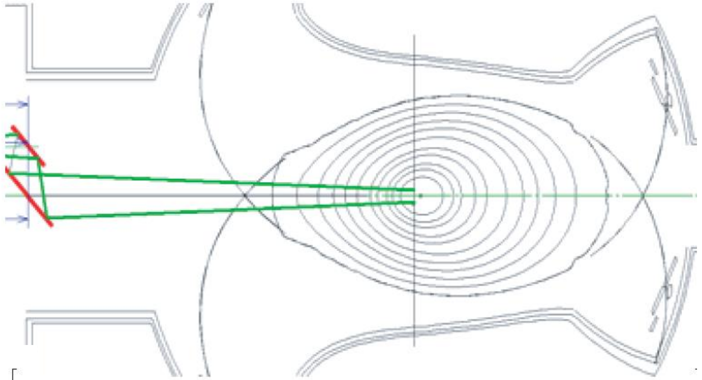

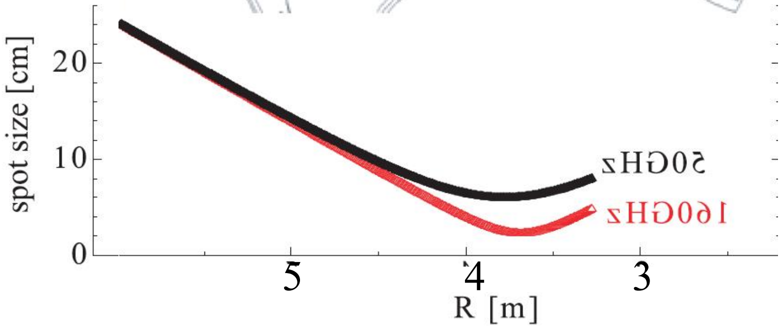

- ✓ Recently, ONLY radiometer is utilized for ECE measurement.
- ✓ Relative calibration using Thomson Scattering signals.

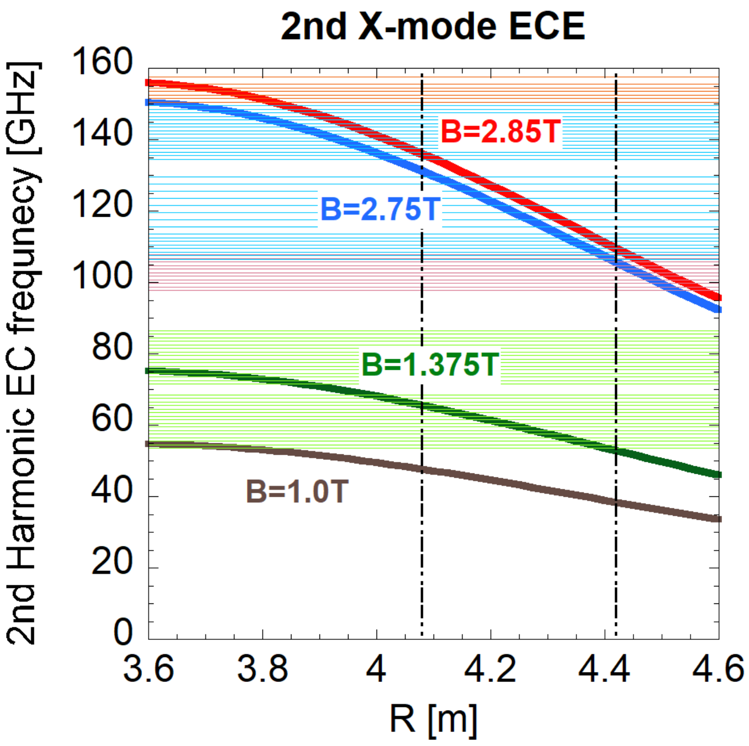

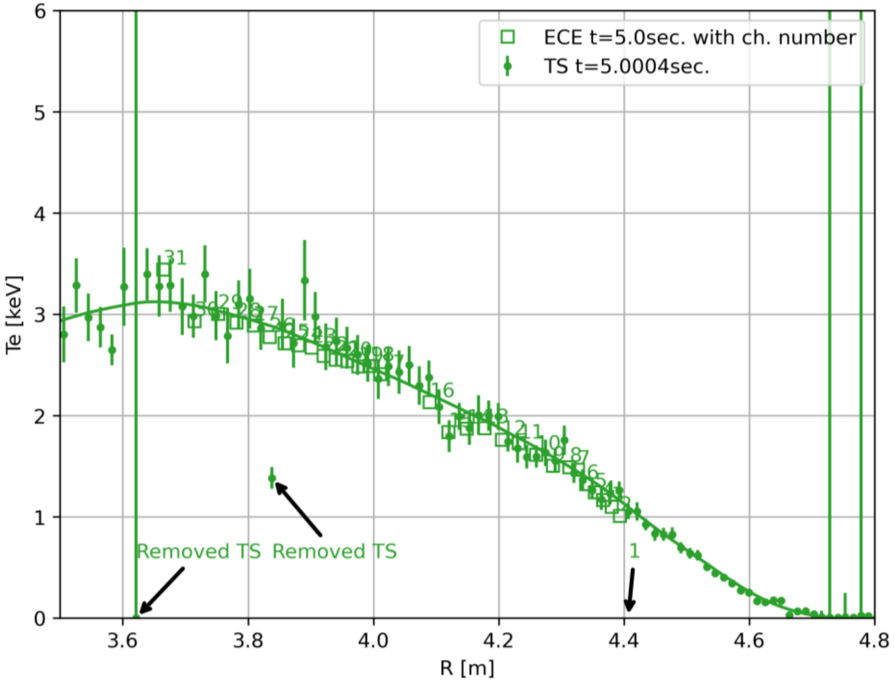

Recent ECE calibration

✓ Example of calibrated ECE radiometer channel.

194421

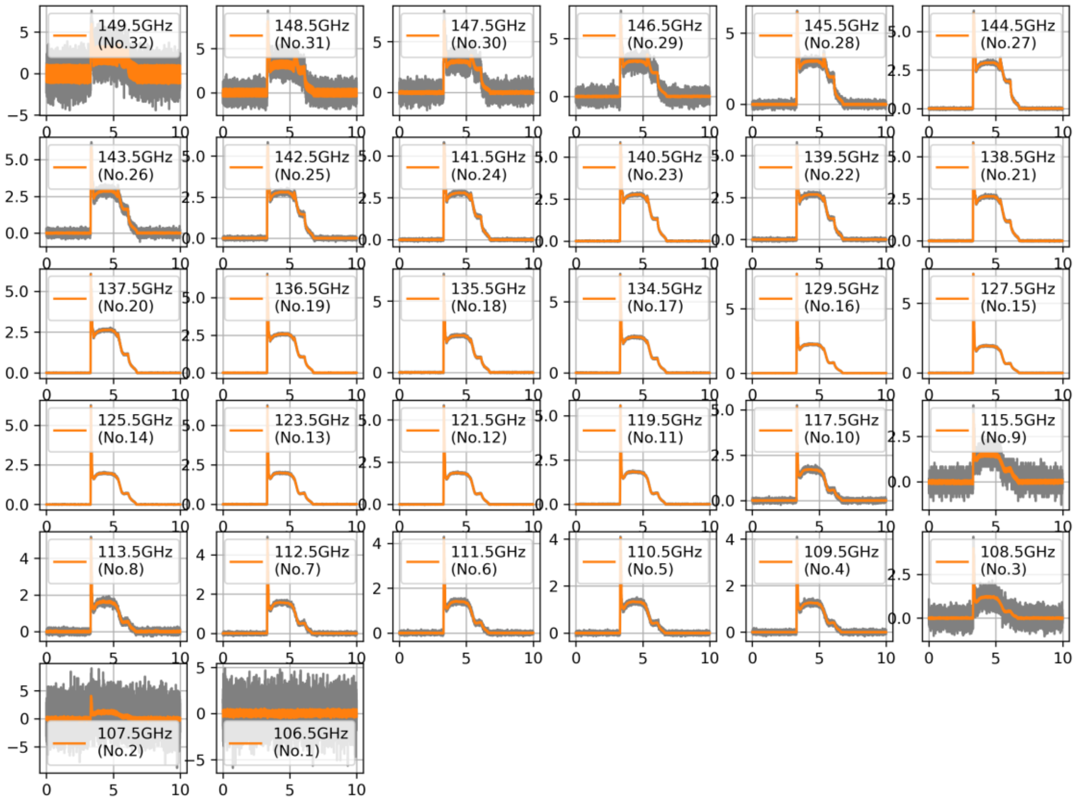

195012

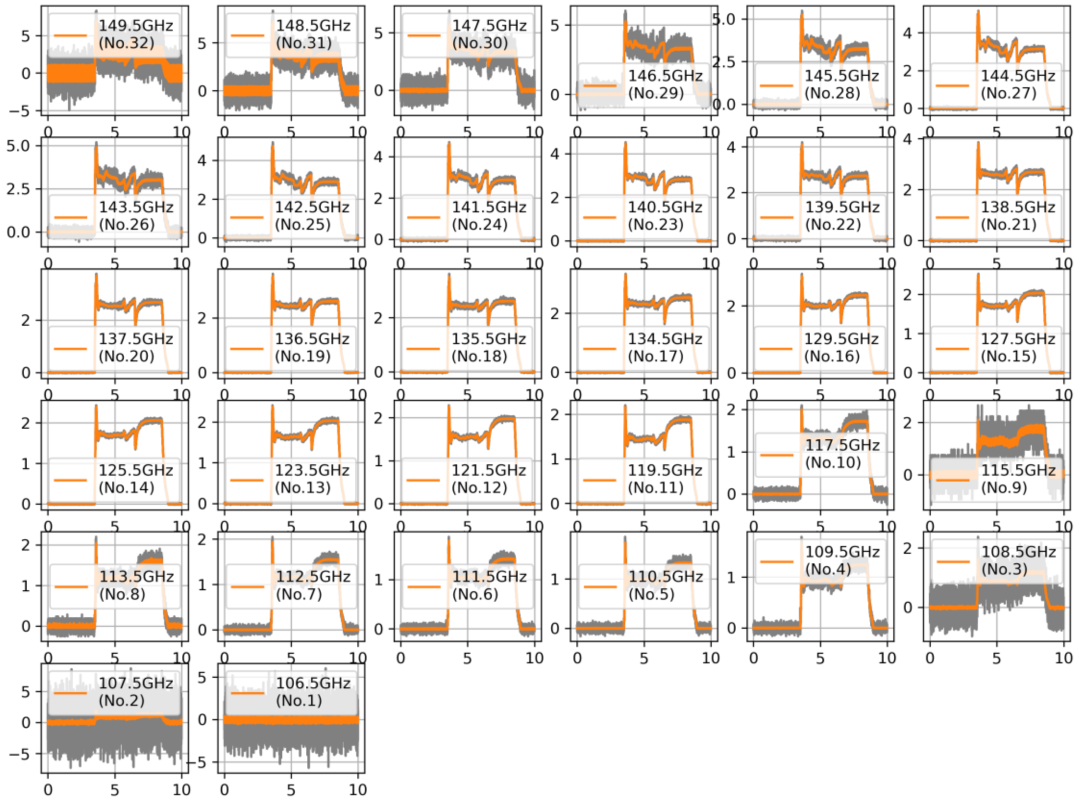

Ref: Thomson scattering in LHD

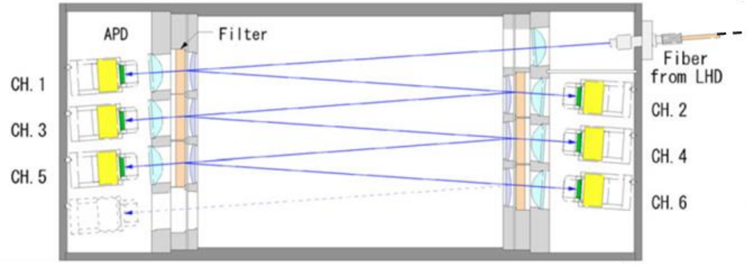

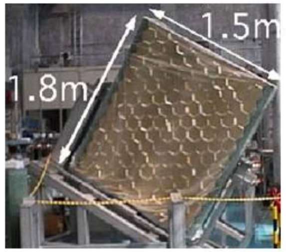

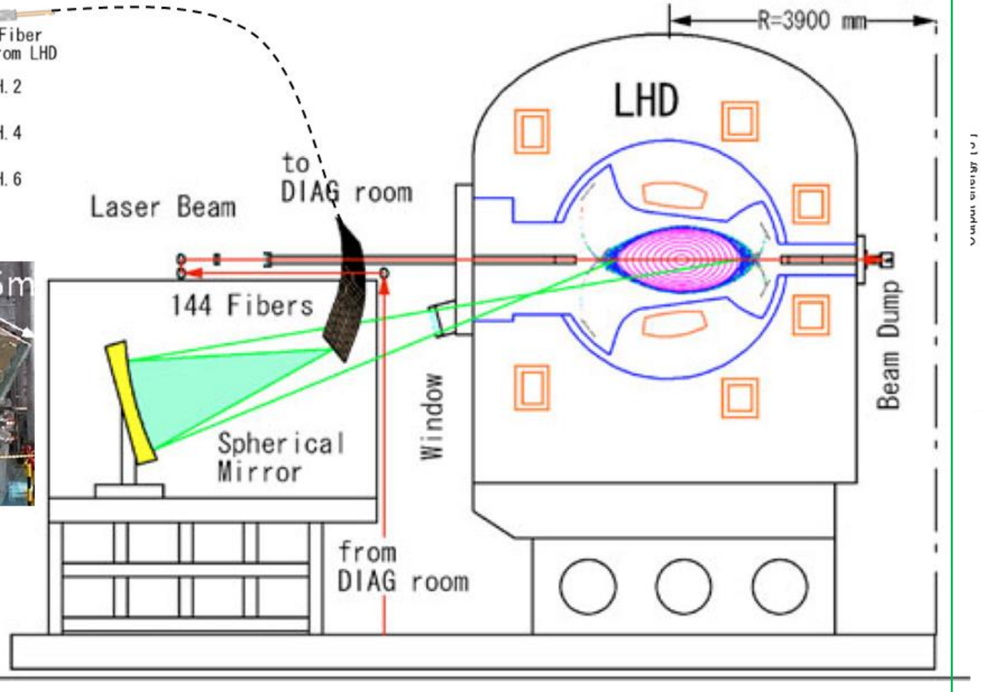

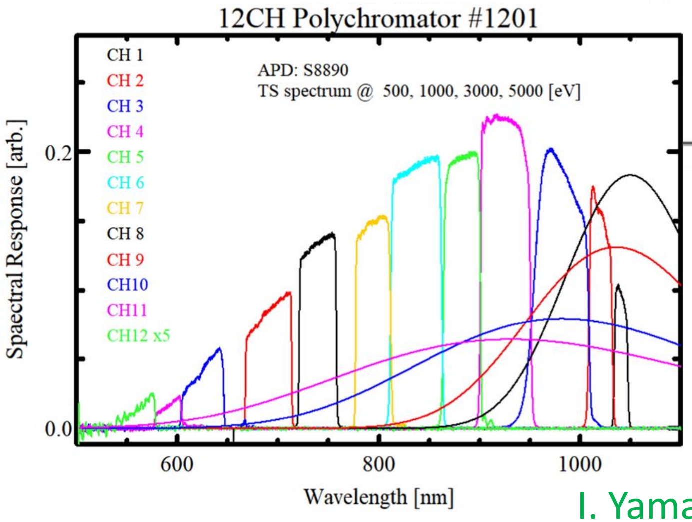

- spatial points: 144 point, resolution: 25mm
- temporal resolution: 10Hz - 130Hz
- measurable temperature : T_e=5eV - 20keV
- measurable density : $n_e=10^{18}$ - 10^{21} m^{-3}

I. Yamada+, *J Fusion Energ* **44**, 54 (2025).

high temporal resolution TS

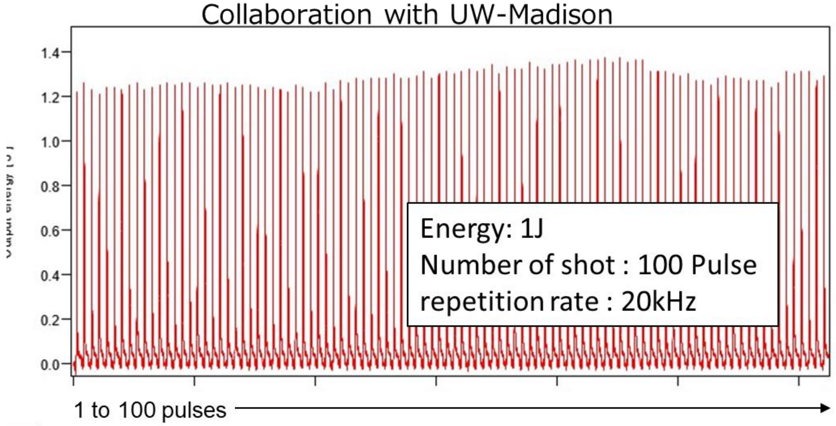

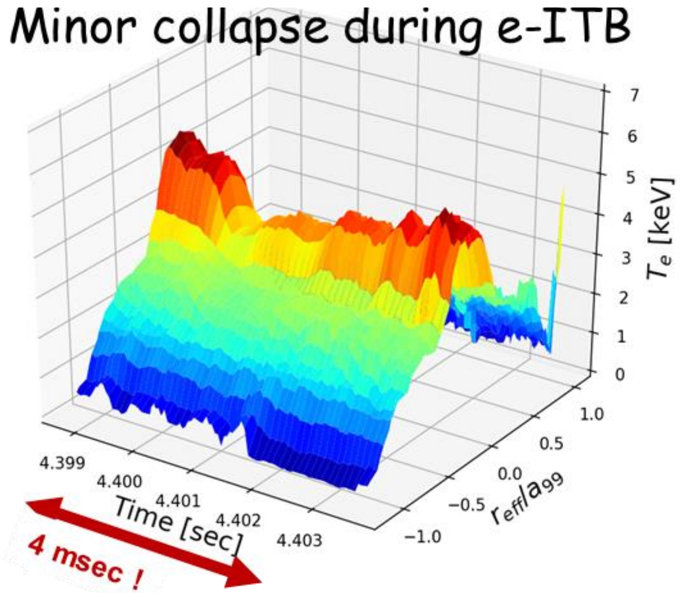

H. Funaba+, *Sci Rep* **12**, 15112 (2022).

Contents

- ECE
  - Previous work
  - Recent work
- Millimeter-wave back-scattering
  - Elimination of back-ground noise
- Phase contrast imaging (Forward scattering)
  - Absolute density fluctuation estimation

Line-of-sight of millimeter-wave back scattering

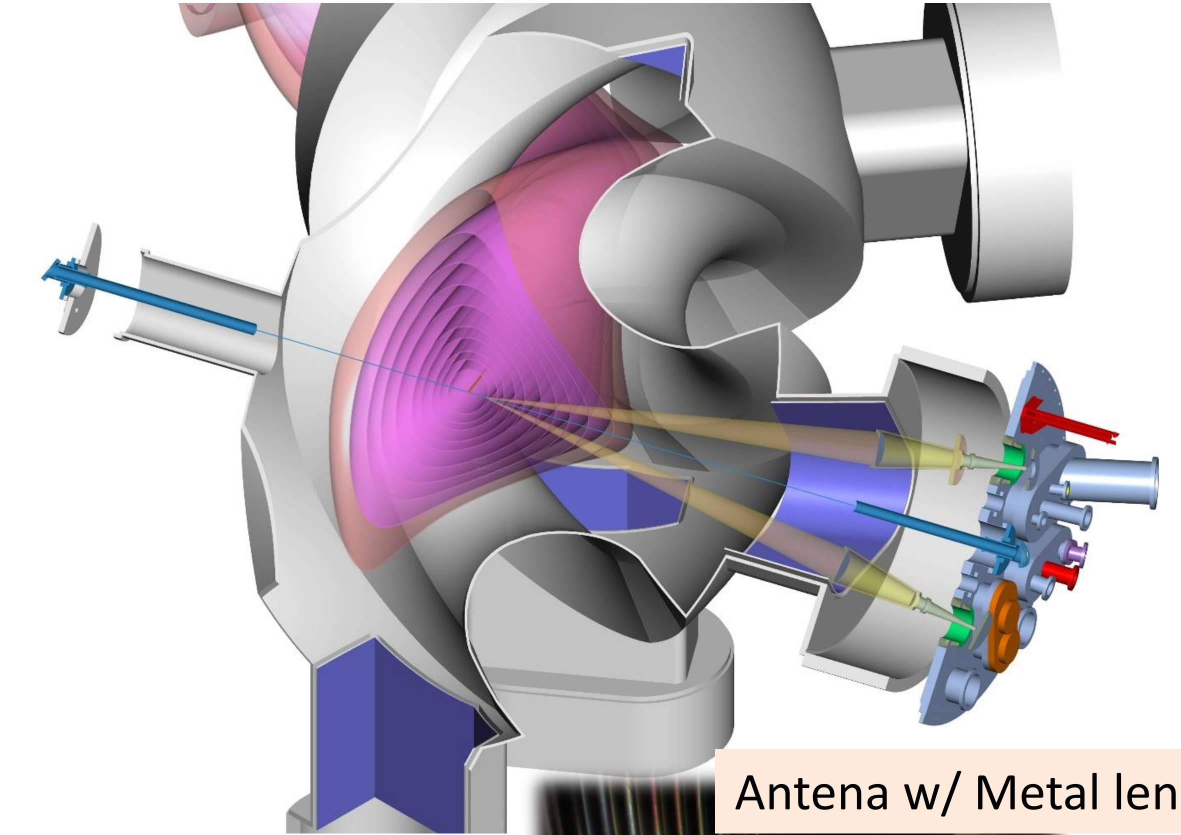

Antena w/ Metal lens

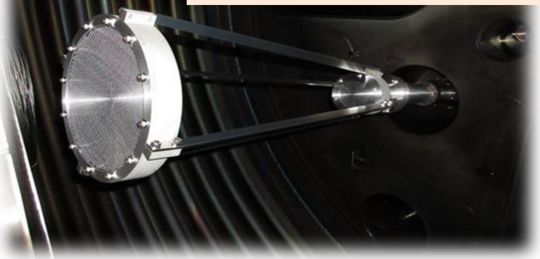

T. Tokuzawa+, Rev. Sci. Instrum. 92, 043536 (2021)

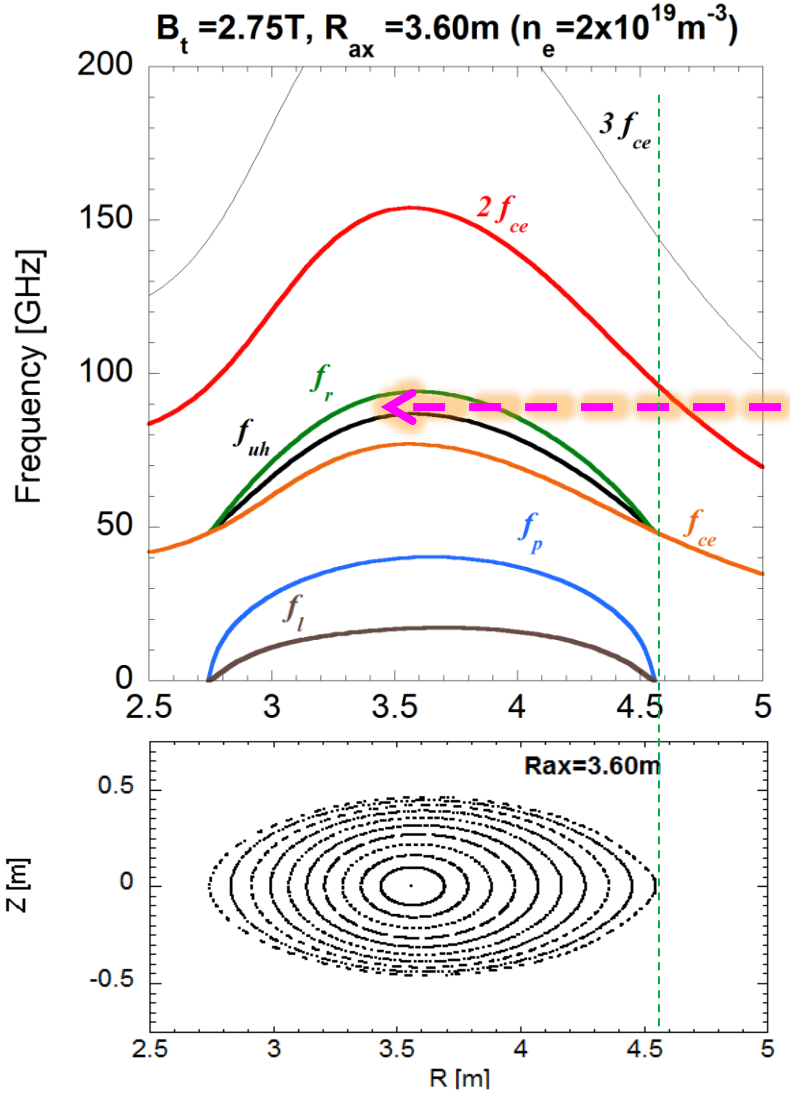

- $2f_{ce}$ layer is located just outside the plasma.
  → 90GHz wave can propagate into the plasma with no absorption.
- In addition, 140GHz System is operation at Bt <2T.

W-band BS system

T. Tokuzawa+, Rev. Sci. Instrum. 92, 043536 (2021)

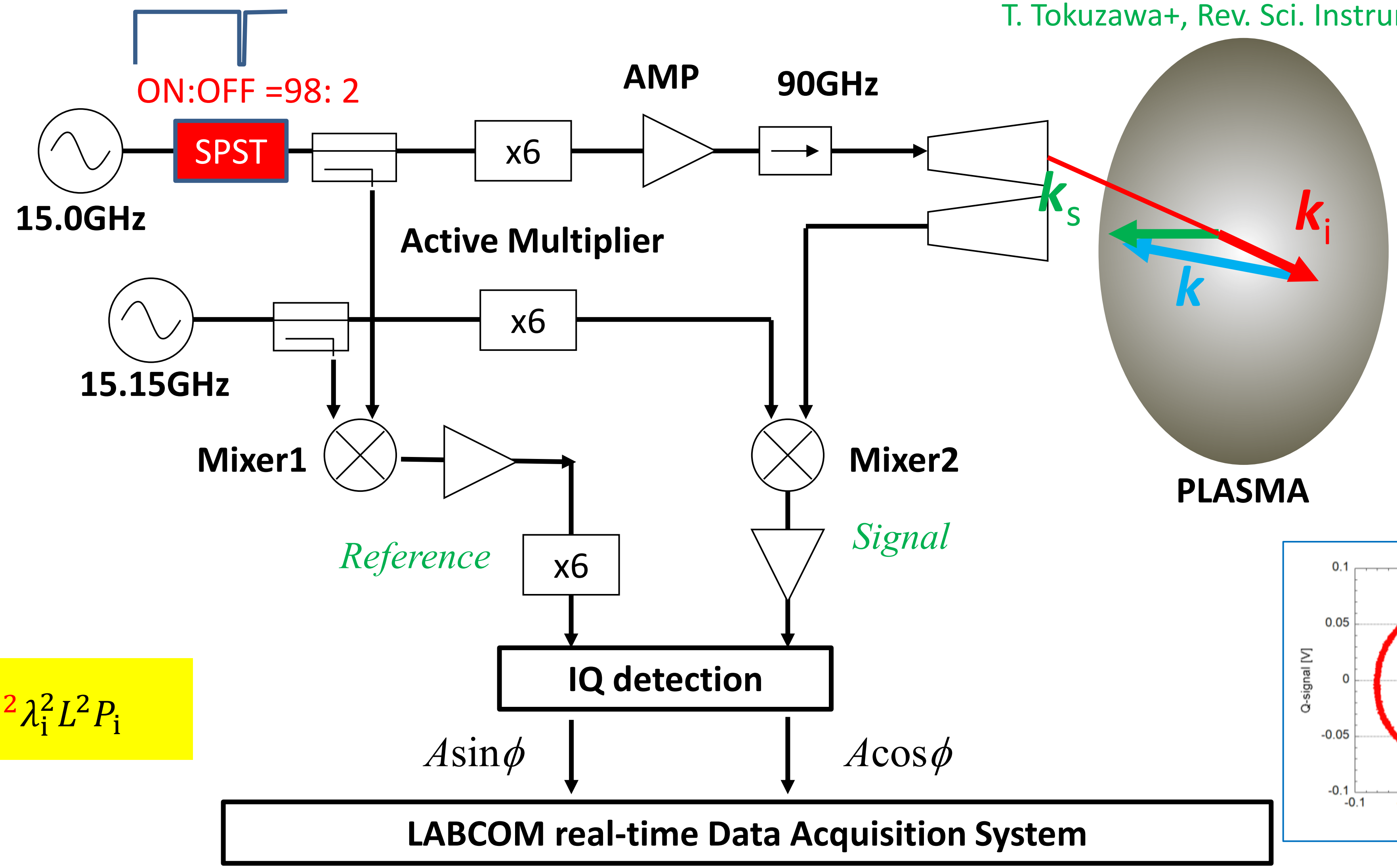

$$P_s = \frac{1}{4} r_0^2 |\widetilde{n_e}|^2 \lambda_i^2 L^2 P_i$$

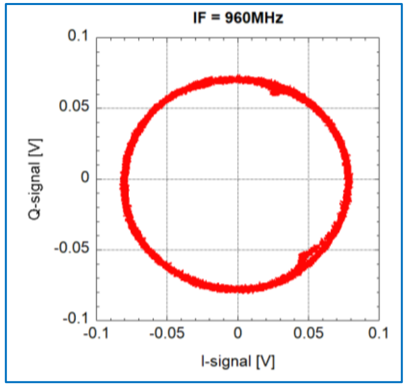

Transmission line (60m)

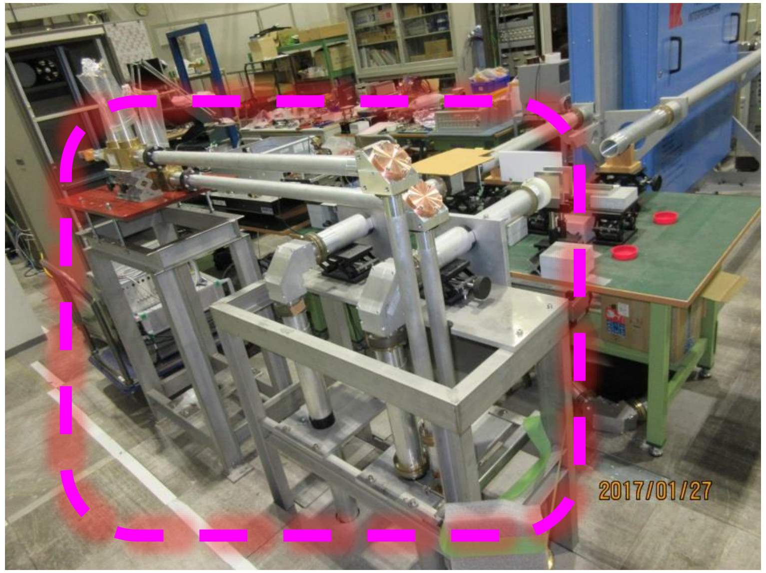

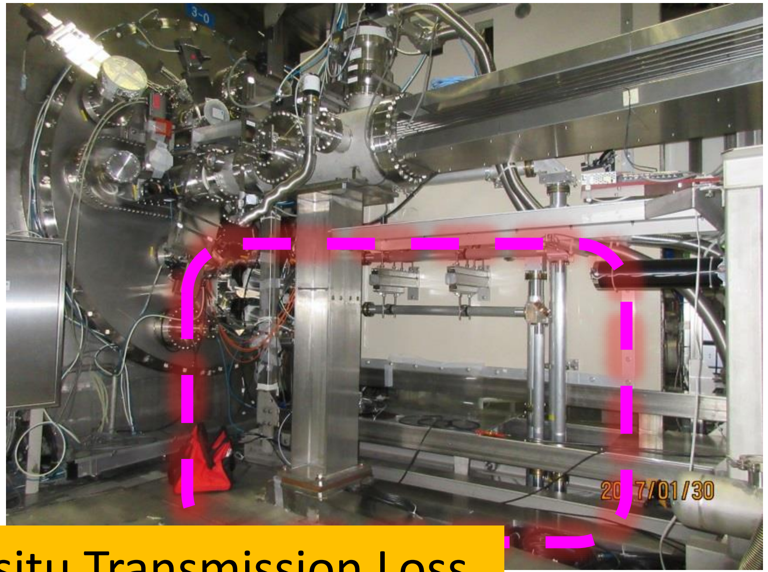

- Designed Loss estimation (1.5”) for receiver

Frequency [GHz]	60	80	120	160	200	220
Loss [dB/ 50m]	1.29	0.40	0.11	0.066	0.075	0.105

- 2.5” (Launcher) : -6dB@90GHz

In-situ Transmission Loss in W-band (1.5”)

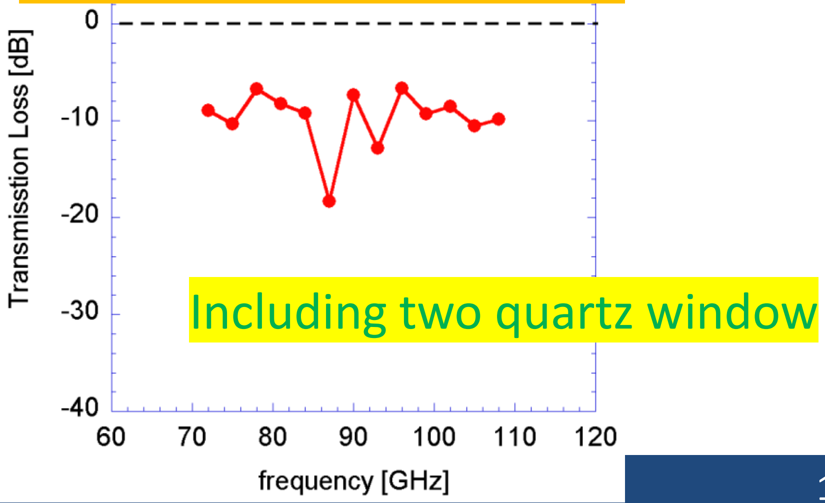

Modulation for the estimation of background noise

I-signal
Q-signal
control

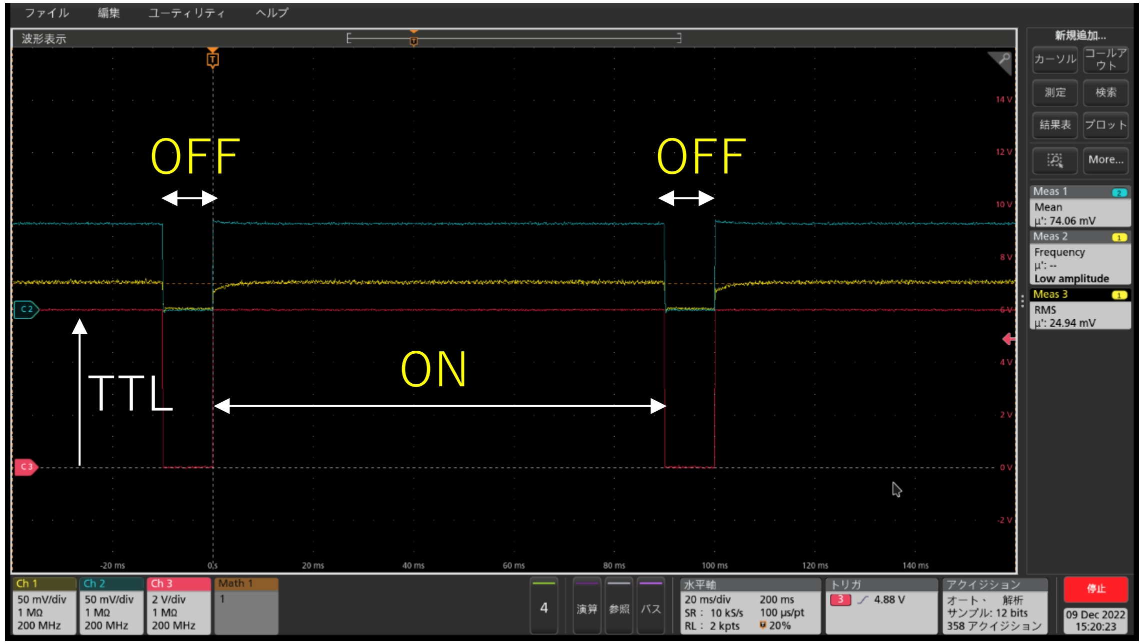

TTL signal is used for switching

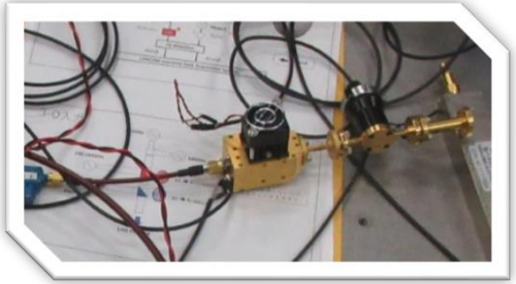

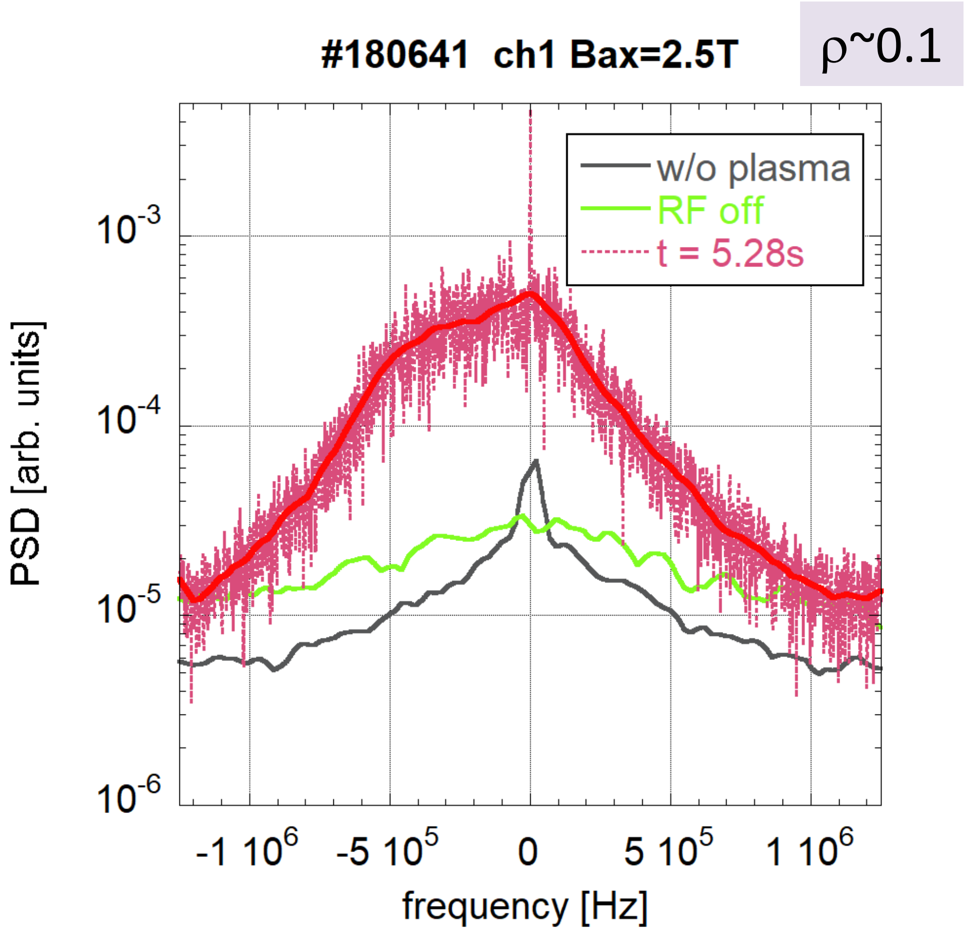

Estimation of noise components

- ✓ It is assumed background noise of BS system is estimated by linear regression with ECE intensity

$$I_{BS}(t) = I_{turb}(t) + n_{BS}(t)$$
$$= I_{turb}(t) + n_{EC}(t) + n_{th}$$
$$= I_{turb}(t) + \alpha I_{EC}(t) + n_{th}$$

$$n_{BS} = n_{EC} + n_{th}$$

$$n_{EC} = \alpha I_{EC}$$

$$n_{BS} = \alpha I_{EC} + n_{th}$$

n_{BS} : background noise
n_{EC} : ECE noise (related by ECE radiation intensity I_{EC})
n_{th} : offset noise (electric circuits noise)

T. Nasu+, Plasma and Fusion Research **20**, 1202056 (2025)

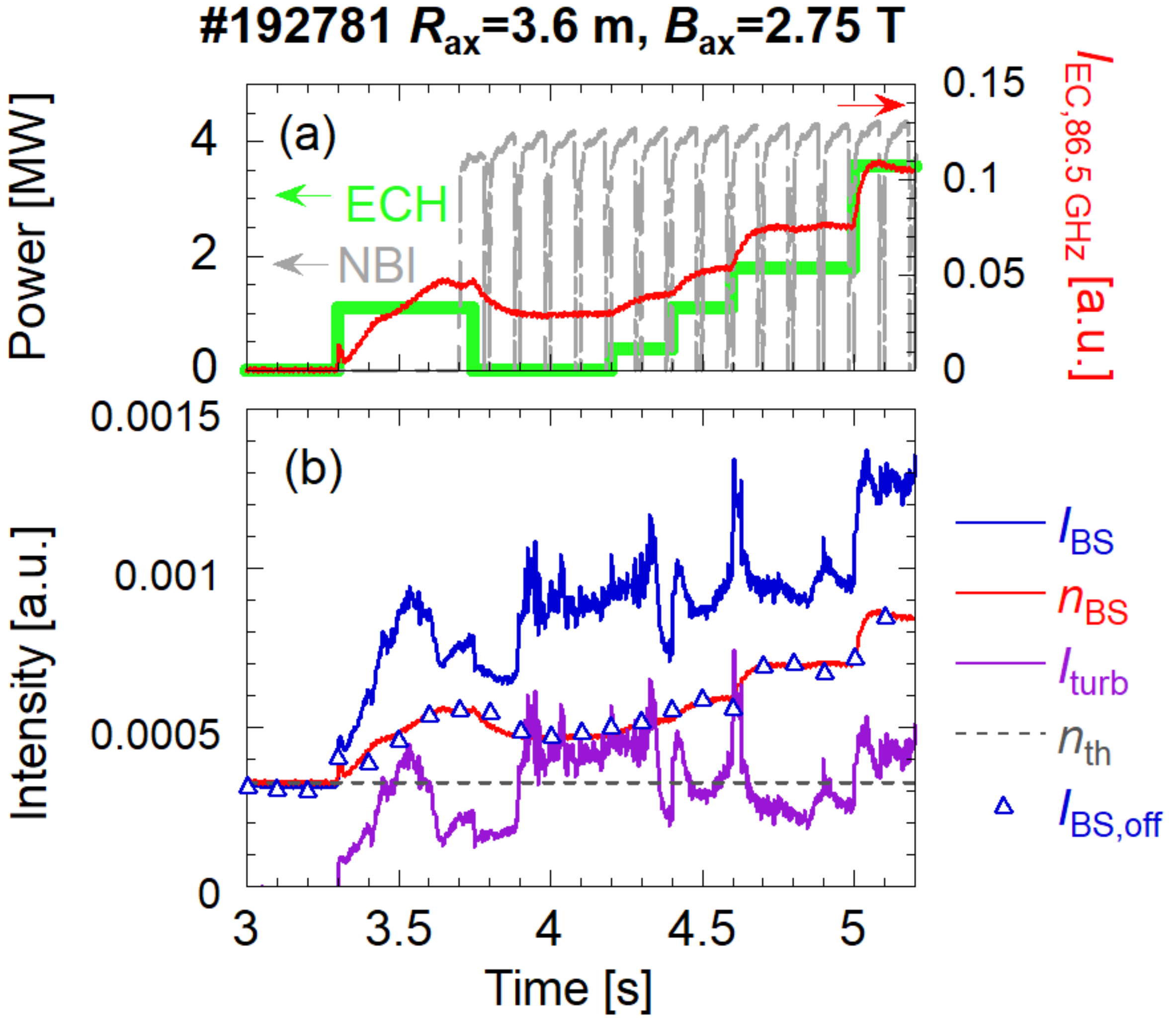

Contents

- ECE
  - Previous work
  - Recent work
- Millimeter-wave back-scattering
  - Elimination of back-ground noise
- Phase contrast imaging (Forward scattering)
  - Absolute density fluctuation estimation

2D PCI (phase contrast imaging) in LHD

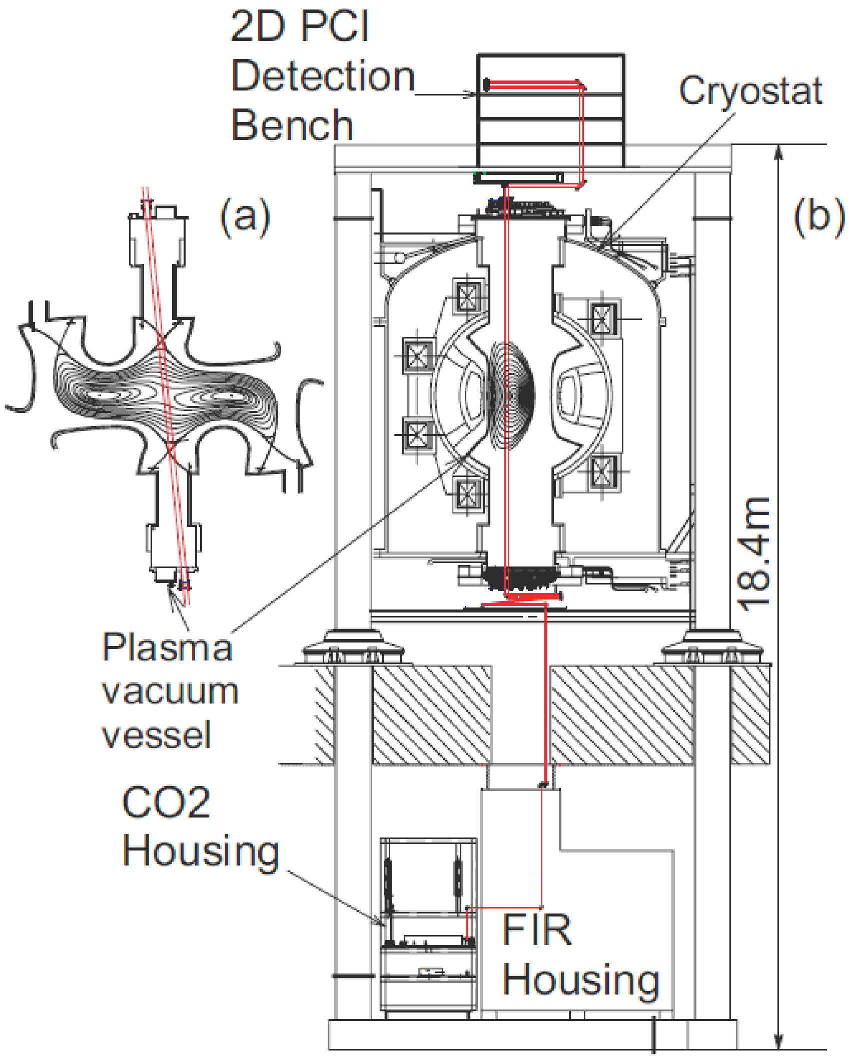

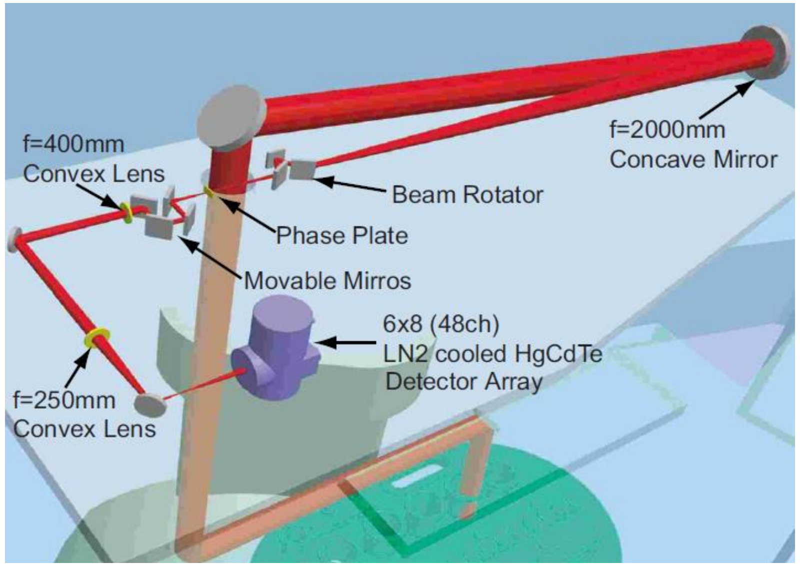

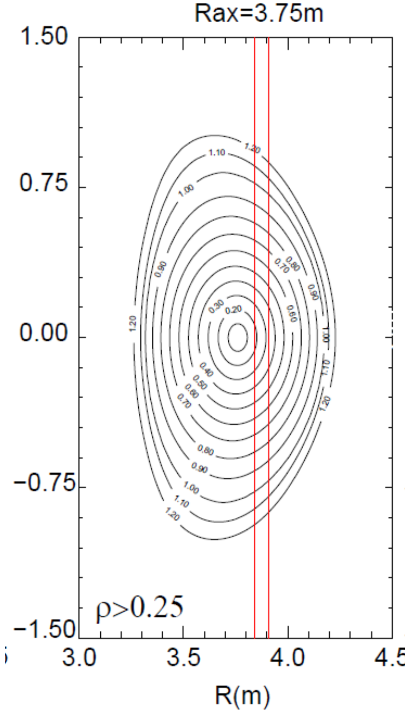

- k=0.1~0.8mm^{-1}
- f=5~500kHz
- Spatial resolution δρ=10~30% of minor radius.
- Almost entire region of turbulence profile can be measured.
- Mainly, poloidal dominated k is measured (measured k can be distinguished up-down symmetry).

K. Tanaka+, Rev. Sci. Instrum. 79, 10E702 (2008)

Principle of PCI

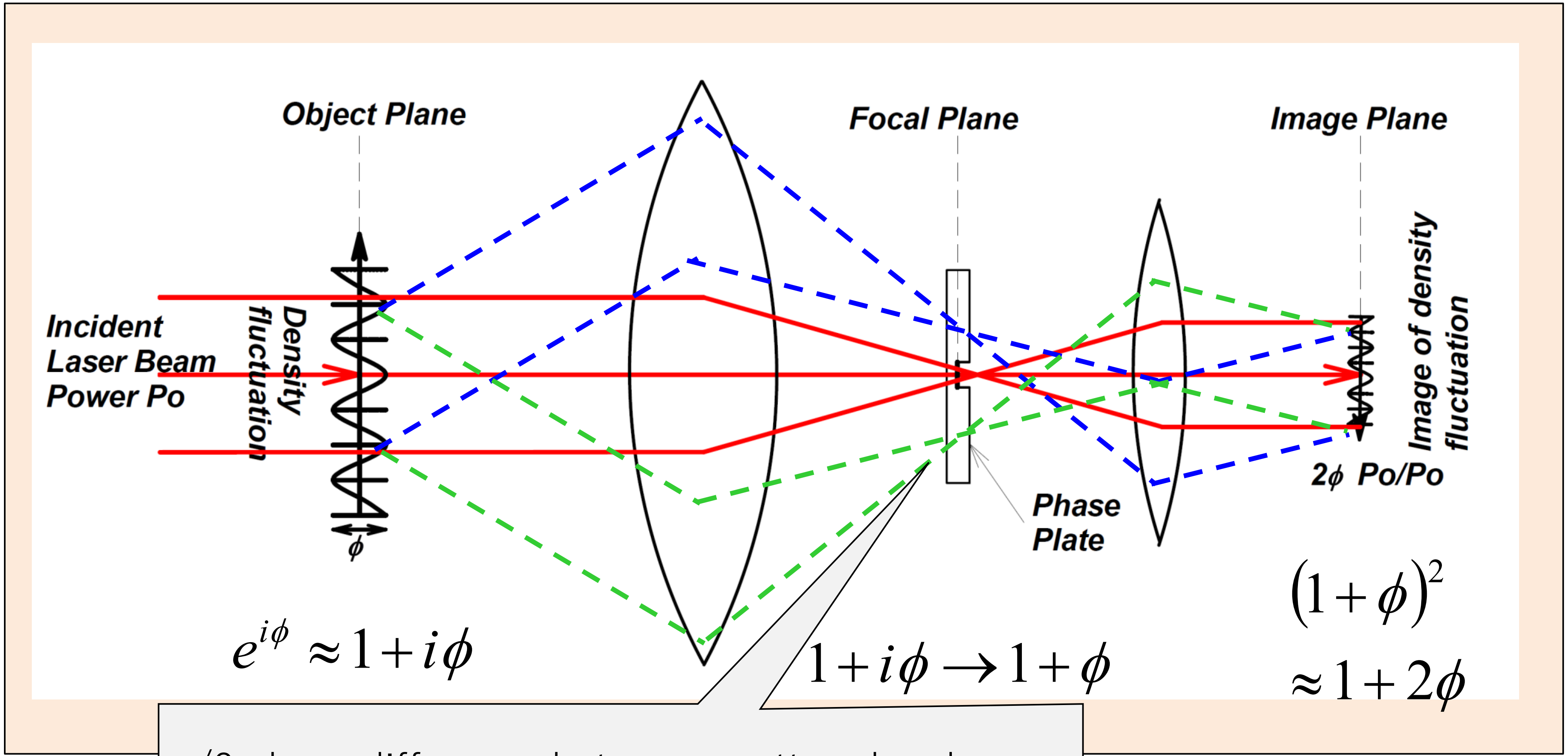

$\pi/2$ phase difference between scattered and transmitted light. This converts phase modulation to intensity modulation

Decomposing into 2D k spectrum using by magnetic shear

K. Tanaka+, Rev. Sci. Instrum. 79, 10E702 (2008)

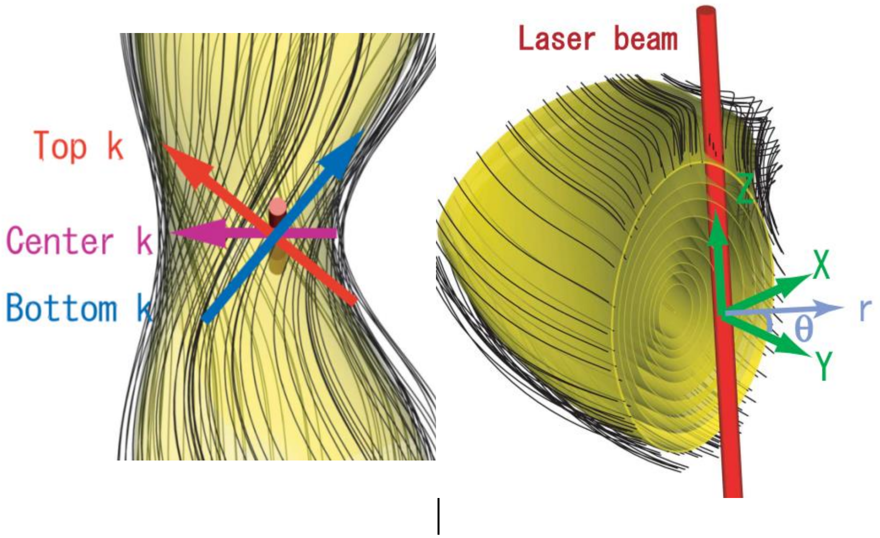

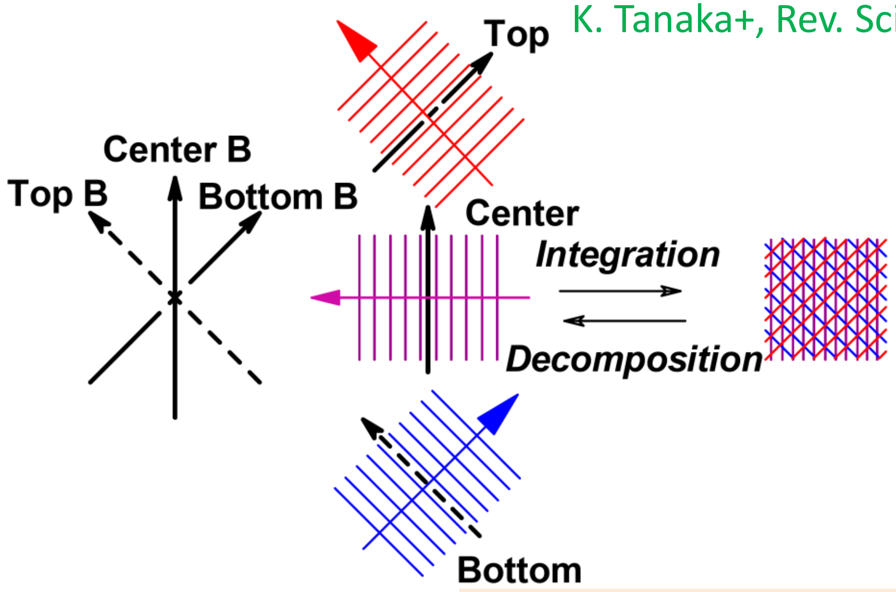

$S(k_x,k_y)$ in Cartesian Corrd.

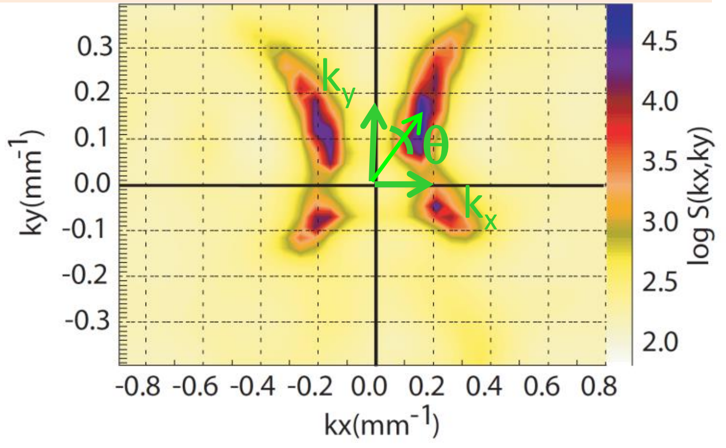

$$k = \sqrt{{k_x}^2 + {k_y}^2}$$

$$\theta = \tan^{-1}\left(k_y / k_x \right)$$

$S(k,\theta)$ in Polar Corrd.

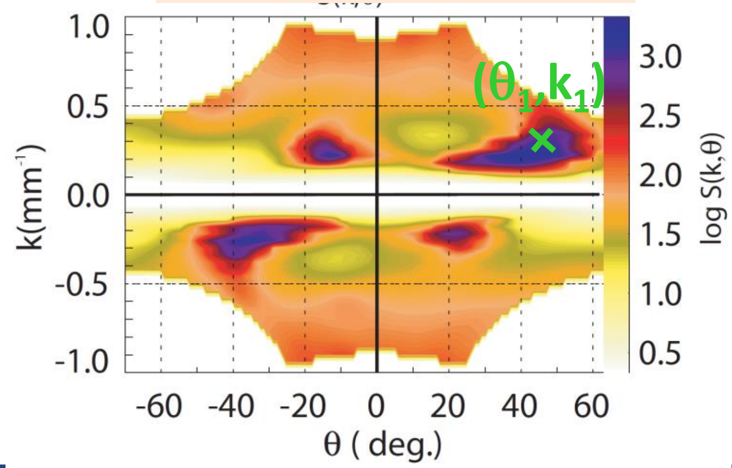

Detector characteristic is obtained at test bench

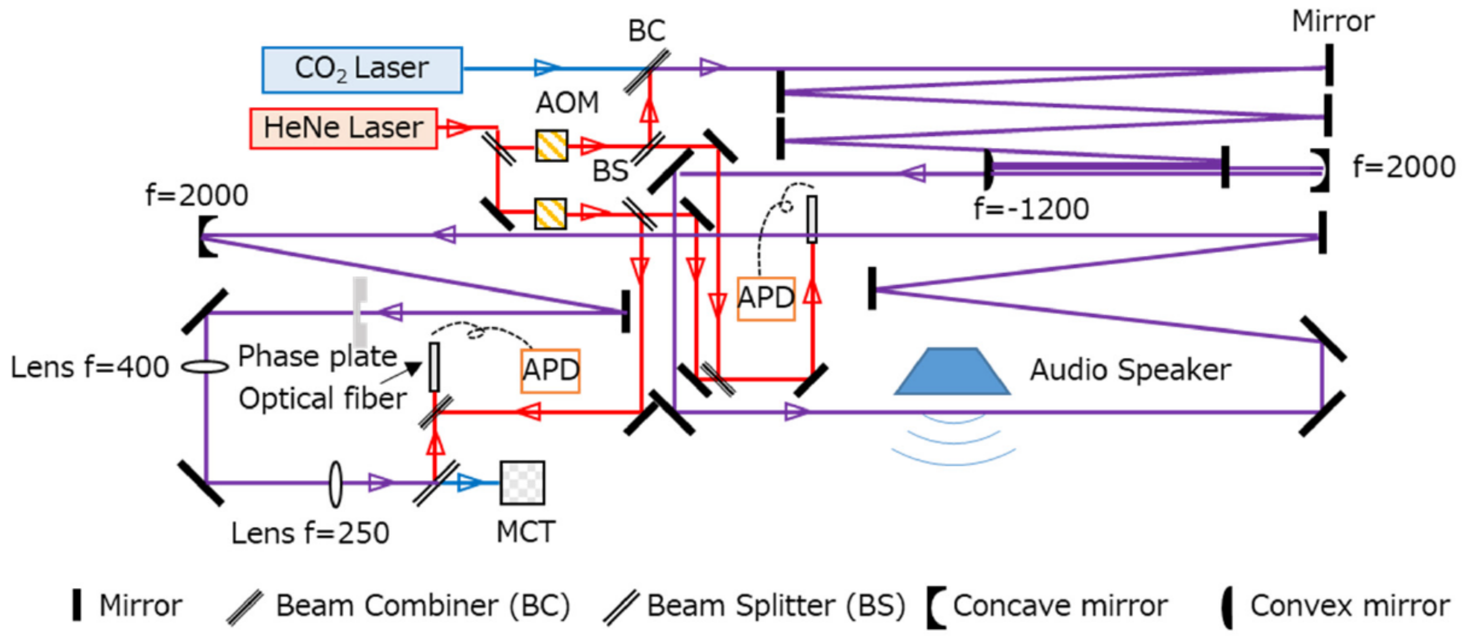

Figure 2. CO_2-PCI and HeNe-HI optics layout for bench test. The blue line and the red line indicate CO_2 laser and HeNe laser, respectively. The purple line indicates a part which HeNe laser is coaxially superposed on CO_2 laser.

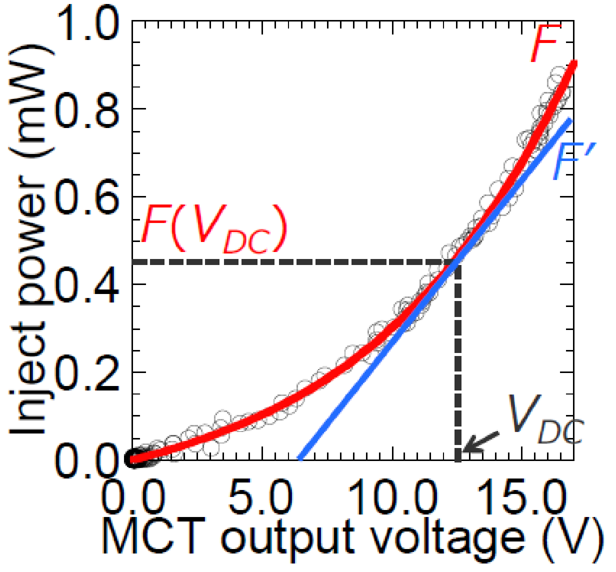

Figure 2. I-O characteristics of 2D-MCT ch21.

T. Kinoshita et al 2020 JINST 15 C01045
T. Kinoshita et al 2023 JINST 18 C11009

Calibration process

The absolute values of the turbulence profile is evaluated according to figure 6 and the following steps.

1. The absolute value of the line-integrated electron density fluctuation amplitude $\tilde{n}_e L(\mathrm{m}^{-2})$ in each channel are evaluated as shown in figure 6(a). Here, the effective value of the periodic fluctuation signal is assumed to be the amplitude of each channel.
2. The electron density fluctuation profile $\tilde{n}_e(\mathrm{a.u.})$ is evaluated in arbitrary units using the magnetic shear technique as shown in figure 6(b).
3. The electron density fluctuation profile evaluated in arbitrary units is line-integrated along the line-of-sight. Then, the line-integrated electron density fluctuation amplitude $\tilde{n}_e L(\mathrm{a.u.})$ is evaluated based on eq. (2.5).
4. The absolute value conversion factor is obtained by dividing the average value among channels of $\tilde{n}_e L(\mathrm{m}^{-2})$ by $\tilde{n}_e L(\mathrm{a.u.})$.
5. The conversion factor is multiplied by $\tilde{n}_e(\mathrm{a.u.})$ to evaluate the absolute value $\tilde{n}_e(\mathrm{m}^{-3})$ of the electron density fluctuation profile.
6. The absolute calibration error is evaluated based on the standard deviation among channels of $\tilde{n}_e L(\mathrm{m}^{-2})$.

$$\tilde{n}_e L = \frac{4c^2 \pi \epsilon_0 m_e}{e^2} \frac{\tilde{\phi}}{\lambda_i} \quad (2.5)$$

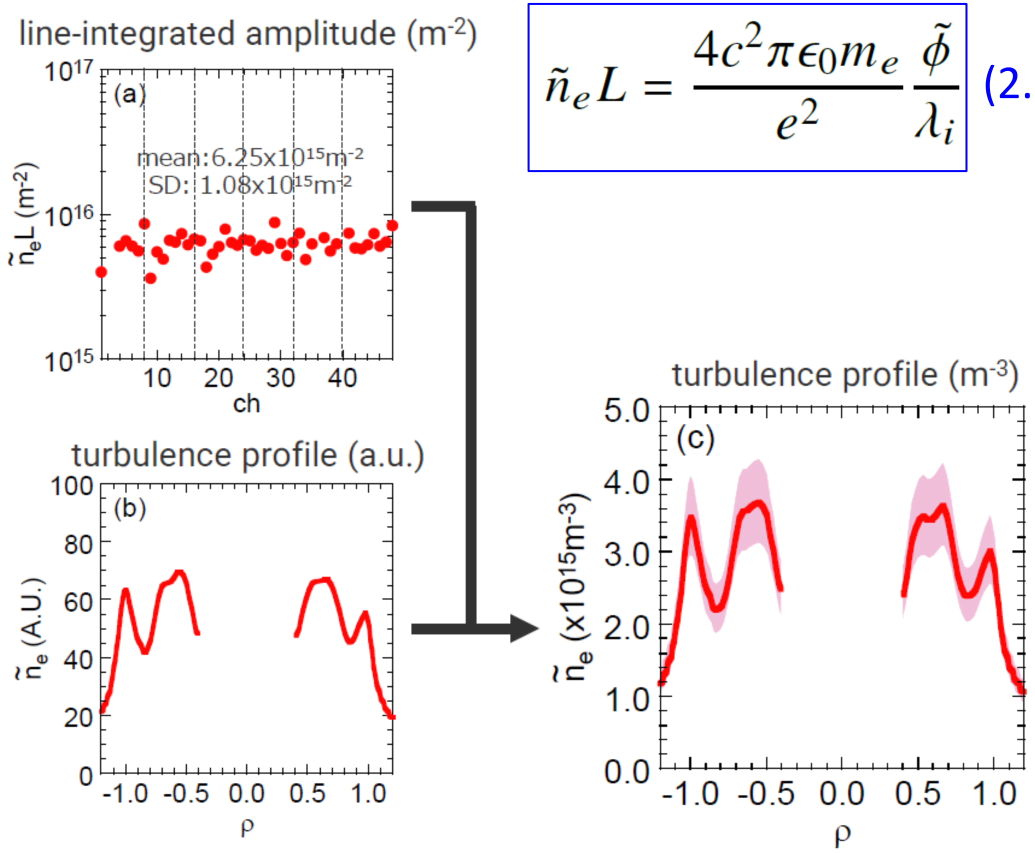

Figure 6. Procedure to evaluate the absolute value of the electron density fluctuation distribution. The normalized radius ρ is defined as the effective minor radius normalized by radius a_{99}, where the electron pressure inside a_{99} is equal to 99% of the total electron pressure [22].

T. Kinoshita et al 2023 JINST 18 C11009

Summary

Calibration technique of old/recent ECE, millimeter-wave back-scattering, forward-scattering PCI in LHD are discussed.

- ECE
  - Previously absolute calibration to Michelson spectrometer.
  - Recently relative calibration to radiometer using TS.
- Millimeter-wave back-scattering
  - Elimination of back-ground noise
- Phase contrast imaging (Forward scattering)
  - Absolute density fluctuation estimation

Thank you for your attention!